First Principles Study of the Adsorption Structure of Ethylene on Ge(001) Surface

X. L. Fan,*,† C. C. Sun,† Y. F. Zhang,‡ and W. M. Lau§

School of Material Science and Engineering, Northwestern Polytechnical University, 127 YouYi Road West, Xian 710072, Shaanxi, China, Department of Chemistry, Fuzhou University, Fuzhou 35002, China, and Surface Science Western, University of Western Ontario, London, Ontario, Canada N6A 5B7

Received: September 7, 2009; Revised Manuscript Received: December 9, 2009

The adsorption of ethylene on the Ge(001) surface is investigated by the first principles density-functional calculations. Our total energy calculations and reaction path investigations clarify the relative importance of various adsorption configurations at 0.5 and 1.0 monolayer adsorption coverage. The results are consistent with the experimental data in the literature in that both the di-σ and paired-end-bridge configurations are the favorable structures on Ge(001). In addition, our calculation results clarify that having di-σ-bound ethylene and end-bridge-bound ethylene next to each other is unfavorable. Such new results imply that although di-σ-bound ethylene and end-bridge-bound ethylene may coexist on Ge(001), phase separation will occur to form adsorbate domains. The electronic structures have also been studied, and the band structure calculations show that both the di-σ and end-bridge models at 0.5 monolayer are semiconducting with a small band gap of $\sim$0.4 eV, which is slightly larger than the band gap of the virgin Ge(001) $p(2 \times 2)$ surface. Increasing the coverage to 1.0 monolayer further widens the band gap in both cases. The results thus rule out the past postulation that ethylene adsorption may turn Ge(001) to metallic.

1. Introduction

The chemistry and physics of hydrocarbon adsorption on elemental and compound semiconductors has emerged as an important subject in the development of molecular microelectronic and optoelectronic devices because the chemical adsorption structure and dynamics govern the device fabrication and stability, while the electronic structure governs the device operation.[1] Since the assembly of unsaturated hydrocarbons into a molecular layer also gives rise to a HOMO−LUMO band structure with conductivity varying from metal-like to semiconducting, studying such an assembly on conventional semiconductors indeed makes a quantum jump of the scope of the science of heterojunction device systems. Ethylene, as the simplest unsaturated hydrocarbon, has been considered as the prototype molecule to study the science of these systems.

It is well-understood that the Si dimer is the reactive center on the Si(001) surface; thus, both the intradimer and interdimer adsorption products are possible for C_2H_4/Si(001). The intradimer di-σ model has the two C atoms of the ethylene bonded to the two Si atoms on top of a single surface dimer, and the interdimer end-bridge model has the two C atoms bonded to the two Si atoms on the neighboring side of two adjacent dimers along the dimer axis. In all previous experimental works,[2−7] ethylene molecule is observed to adsorb on a single Si dimer by the intradimer di-σ configuration. The bridge geometry has never been observed. For the adsorption of ethylene on Ge(001), a recent study[8] using the techniques of temperature programmed desorption (TPD) and scanning tunneling microscopy (STM) reports on the experimental observation of both the di-σ and paired-end-bridge configurations in which an additional C_2H_4 molecule adsorption makes the end-bridge structure to be paired. The di-σ configuration of Ge(001) has also been studied theoretically, with the results compared to those on Si(001).[9,10] It is interesting that the theoretical study of the end-bridge configuration by Miotto et al. suggests that the adsorption structure is metallic and is chemically unstable.[9] This study also suggests that the surface states in the gap region are mainly localized on the adsorbed ethylene. These suggestions bear very significant technological implications because they mean that adsorption of ethylene will give a high surface conductivity. It is thus important to examine them carefully.

In the present study, both the di-σ and end-bridge configurations at 0.5 monolayer and the paired-di-σ and paired-end-bridge configurations at 1.0 monolayer, as shown in Figure 1, are studied by the first principles method based on density function theory (DFT). Especially, since after the initial adsorption of di-σ or end-bridge ethylene at very low coverage many adsorption configurations other than the homogeneous growth of di-σ or end-bridge coverage are conceivable, we also examine the mixed adsorption of di-σ and end-bridge ethylene. With the optimized adsorption configurations obtained by the total energy calculations, we then calculate the potential energy surfaces along the reaction pathways via different addition mechanisms to study the reaction kinetics of C_2H_4 molecule adsorption. In additional, we compute the electronic band structures and investigate the origin of the surface states in the vicinity of Fermi energy.

2. Calculation Methods

The first principles calculations of this work were performed using the Vienna ab initio simulation package (VASP)[11−14] on the basis of density functional theory. Vanderbilt ultrasoft pseudopotential was applied[15] for the atomic core regions;[16,17] wave functions were expanded in a plane-wave basis set with a cutoff energy of 350 eV. The generalized gradient approximation (GGA)[18] was used for the exchange-correlation potential. The minimum energy path for the adsorption reactions were

* To whom correspondence should be addressed. E-mail: xlfan@nwpu.edu.cn.
† Northwestern Polytechnical University.
‡ Fuzhou University. E-mail: zhangyf@fzu.edu.cn.
§ University of Western Ontario. E-mail: lau22@uwo.ca.

10.1021/jp9086464
Published on Web 01/12/2010

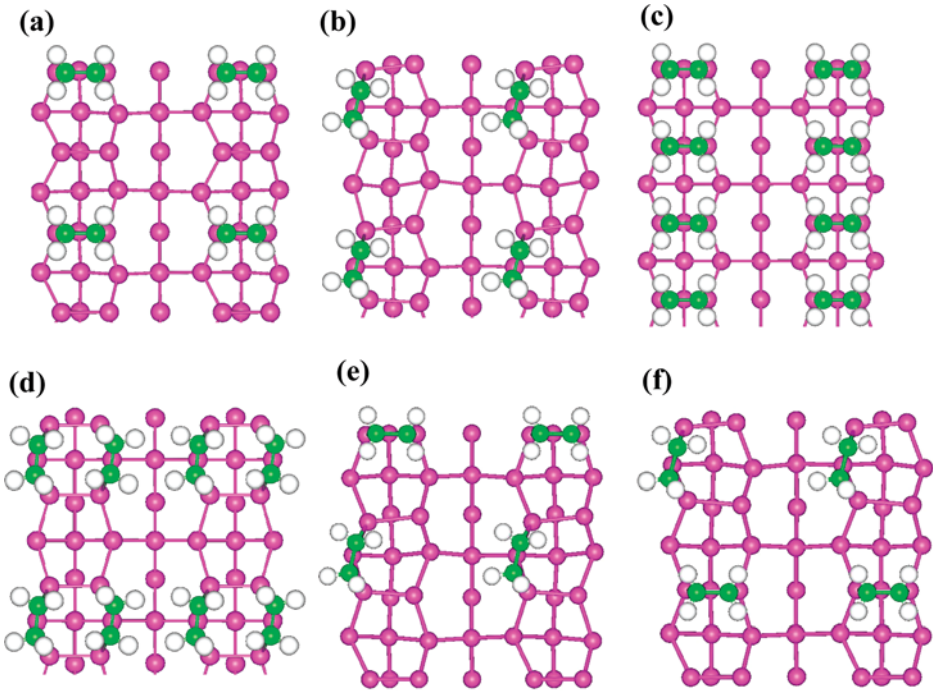

Figure 1. Optimized adsorption configurations for ethylene on Ge(001): (a) di-σ at 0.5 monolayer; (b) end-bridge at 0.5 monolayer; (c) paired-end-bridge at 1.0 monolayer; (d) paired-di-σ at 1.0 monolayer; (e) di-σ ethylene at 0.25 monolayer and then the addition of end-bridge ethylene to a total of 0.5 monolayer; (f) end-bridge ethylene at 0.25 monolayer and then the addition of di-σ ethylene to a total of 0.5 monolayer.

TABLE 1: Computational Results on the Geometric Structures and Binding Energy $E_{ad.}$ (eV) per Adsorbed Molecule for Ethylene on Ge(001)

	0.5 monolayer				1.0 monolayer	
	di-σ	end-bridge	di-σ/end-bridge	end-bridge/ di-σ	paired-di-σ	paired-end-bridge
$E_{ad.}$	1.00	0.90	0.81	0.84	0.97	1.13
Ge−C (Å)	2.05	2.07	2.07	2.06	2.06	2.07
C−C (Å)	1.53	1.54	1.54	1.53	1.53	1.55

mapped out using the nudged elastic band method developed by Jónsson and co-workers.[19,20] Since ethylene has no unpaired electrons, the spin-polarization option is not considered.

The Ge(001) surface was simulated using a repeated slab with eight atomic layers and a vacuum region of 12.94 Å spacing. The top of the slab was modeled by a $p(2 \times 2)$ surface with two asymmetric Ge dimers. The adsorption of one monolayer (1.0 monolayer) of ethylene is defined as the adsorbate molecular surface density and is same as the dimer density of the $p(2 \times 2)$ surface. The bulk lattice constant was determined to be 5.75 Å. The dangling bond of the bottom Ge atoms were saturated by H atoms in the structure optimization, the Ge atoms in the bottom layer of the slab and the hydrogen atoms were fixed to the bulk position, and the other Ge atoms and the adsorbed molecule were fully relaxed. In the total energy calculations, the first Brillouin zone was sampled by a Monkhorst−Pack scheme with $4 \times 4 \times 1$ k-point grids. The electronic band structures have been calculated at 31 k points along the $\Gamma-J-K-J'-\Gamma-K$ symmetry directions of the 2×2 SBZ (surface Brillouin zone).

3. Results and Discussions

3.1. Adsorption Structures. As explained in section 1, we examine in this work the two possible models for ethylene molecule adsorption on Ge(001): the di-σ model and end-bridge model. The following six configurations are included in this examination: (a) homogeneous growth of di-σ adsorption to 0.5 monolayer, as shown in Figure 1a; (b) homogeneous growth of end-bridge adsorption to 0.5 monolayer, as shown in Figure 1b; (c) homogeneous paired-di-σ at 1.0 monolayer, as shown in Figure 1c; (d) homogeneous paired-end-bridge configuration at 1.0 monolayer, as shown in Figure 1d; (e) mixed di-σ/end-bridge configuration formed by adding an end-bridge ethylene next to a di-σ ethylene, to 0.5 monolayer, as shown in Figure 1e; (f) mixed end-bridge/di-σ configuration formed by adding a di-σ ethylene next to an end-bridge ethylene, to 0.5 monolayer, as shown in Figure 1f.

For the first four adsorption configurations of homogeneous adsorption, the Ge(001) $p(2 \times 2)$ surface has been modeled as one unit cell with two asymmetric dimers, and for the last two mixed adsorption configurations, the surface has been modeled as two unit cells with four asymmetric dimers.

We first optimize and compare the atomic structures of di-σ and end-bridge configurations at 0.5 monolayer coverage. The optimized adsorption structures are shown in Figure 1a,b. The calculated adsorption energy and structure parameters for the two structures are given in Table 1, where the C−C bond length is around 1.53 Å, which is around the typical C−C bond length in a sp^3 hybridization configuration of C_2H_6 (1.52 Å). The Ge−C bond length in the end-bridge configuration is 2.07 Å, which is slightly longer than the Ge−C bond length of 2.05 Å in the di-σ configuration. The small difference of the Ge−C bond length between the two binding geometries is reflected by the small difference of their adsorption energies, as we find that

the di-σ configuration is slightly more stable than the end-bridge configuration by 0.1 eV at the coverage of 0.5 monolayer.

The optimized paired-di-σ configurations and paired-end-bridge configuration at 1.0 monolayer coverage are shown in Figure 1c,d, respectively. Both the Ge−C bond length and the C−C bond length are almost the same as those in the adsorption geometries at 0.5 monolayer coverage, as shown in Table. 1. Interestingly the adsorption energy of the paired-end-bridge configuration becomes higher than that of the paired-di-σ configuration at 1.0 monolayer by 0.16 eV. Our respective adsorption energies of 1.0 and 1.13 eV for the di-σ and paired-end-bridge configurations agree well with the corresponding experimental desorption energies of 1.05 and 1.15 eV measured by the temperature programmed desorption technique.[8] In additional, the Ge−C bond length data from our calculations are also consistent with those of the previous calculations.[9,10]

The results for the two mixed configurations at 0.5 monolayer of ethylene are also included in Table 1. We can see both the G-C and C−C bond lengths in the mixed configurations are the same as those in the first four adsorption configurations of homogeneous di-σ and end-bridge adsorption. Energetically, the adsorption energy of the mixed configurations are less than those of homogeneous adsorption by ~0.2 eV, regardless of whether the mixed configuration is initiated by di-σ or end-bridge adsorption.

On the basis of the calculated adsorption energies, we predict that both the di-σ and end-bridge adsorption configurations should coexist under normal experimental conditions due to the small energy differences at both 0.5 and 1.0 monolayer. However, in principle, these results on thermodynamics also imply that one can increase the relative "equilibrium" population of the di-σ configuration at 0.5 monolayer and the paired-end-bridge configuration at 1.0 monolayer by lowering the adsorption temperature. When both the di-σ and end-bridge adsorptions take place on Ge(001), our examination of the mixed configurations further predicts that phase separation will occur and drive the formation of domains of di-σ and end-bridge adsorption in order to minimize the total surface energy. To further examine the kinetic effects on the relative formation probability of these two configurations, we check their formation energy barriers by computing the potential energy surface along the reaction pathways for both of the two configurations.

3.2. Reaction Kinetics. ***3.2.1. General Description of the Asymmetric and Symmetric Addition Pathways.*** Adopting the methodology in the previous studies of the reaction pathways of C_2H_4/Si(001),[21,22] we have computed the following reaction pathways of C_2H_4/Ge(001):

(a) The asymmetric addition pathway with a π dative bond linking the ethylene molecule to the "down"-Ge atom of a Ge−Ge dimer is a highly probable route because the "down"-Ge atom of a Ge−Ge dimer is known to be electron-deficient and because the ethylene molecule can access this route with no strict alignment requirement of the ethylene molecular axis in its arrival trajectory relative to the Ge−Ge dimer. Once this intermediate is formed, there are two possible pathways for more stable chemisorption: Path I describes the formation of the di-σ configuration, and path II leads to the formation of the end-bridge configuration. For examining the homogeneous paired-adsorption to 1.0 monolayer, we calculate the energetic data for the addition of one more ethylene to the homogeneous adsorption at 0.5 monolayer by keeping the homogeneous adsorption condition. For example, the results for the paired-di-σ configuration at 1.0 monolayer describe the reaction pathway for the addition of one di-σ ethylene to each unit cell of di-σ adsorption at 0.5 monolayer. For examining the mixed adsorption cases, we use the unit cell of di-σ (end-bridge) adsorption at 0.25 monolayer and add one end-bridge (di-σ) ethylene next to the di-σ (end-bridge) ethylene already present in the unit cell. The mixed adsorption cases in this work thus all have a coverage of 0.5 monolayer.

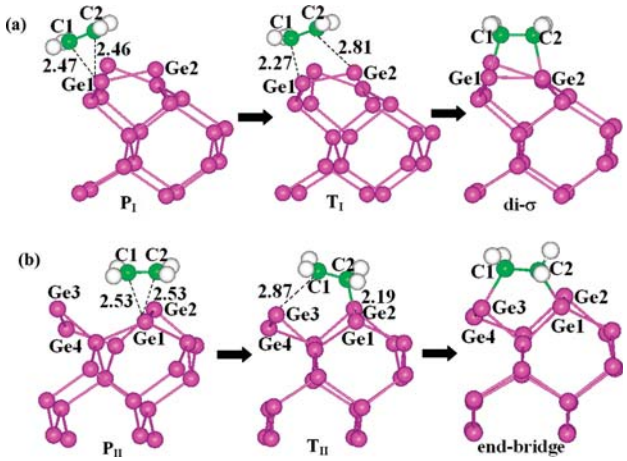

Figure 2. Atomic geometries of the π-complex precursor (P), transition (T), and chemisorption (C) states for the adsorption of C_2H_4 on Ge(001) surface along (a) path I (asymmetric addition reactions leading to the di-σ structure) and (b) path II (asymmetric addition reactions leading to the formation of the end-bridge structure).

(b) The symmetric concerted [2 + 2] cyclo-addition pathway is included for the examination of the possible impact of this route. Like the asymmetric route, this symmetric route can also branch out to paths to the di-σ and end-bridge configurations: Path III to the di-σ configuration, path IV to the end-bridge configuration, and subsequently the paired-adsorption configurations. Similar to the situation of the asymmetric addition cases, the mixed adsorption is also examined.

3.2.2. Energetics of the Asymmetric Reaction Pathways. As displayed in Figure 2a,b, the precursor states labeled as P_I and P_{II}, respectively, describe the asymmetric addition of ethylene leading to the di-σ and end-bridge structures. The P_I state is a little more stable than the P_{II} state by 0.05 eV. Correspondingly, the C−Ge distances in the P_I state are a little smaller than those in the P_{II} state. By using the NEB method, we have found the minimum energy paths from the precursor states to the di-σ and end-bridge structures, labeled as I and II. The atomic geometries of the precursor (P), transition (T), and chemisorptions (C) states on reaction paths I and II are displayed in Figure 2a,b, and the corresponding adsorption energies are given in Table 2.

For the homogeneous adsorption cases to 0.5 monolayer, along path I, the respective adsorption energy of the P_I and T_I states are 0.40 and 0.17 eV; thus, the reaction barrier from P_I to the di-σ phase is 0.23 eV. In comparison, along path II, the corresponding adsorption energies for P_{II} and T_{II} are 0.35 and 0.16 eV, and the reaction barrier for the end-bridge structure is 0.19 eV. According to the previous calculation results,[22,23] the adsorption energies for the P_I and P_{II} states on the Si(001) surface are both about 0.41 eV. Our calculated adsorption energy for the P_I and P_{II} states on Ge (001) are a little smaller than those on the Si(001) surface, while our calculated reaction barriers are slightly higher than those on the Si(001) surface.[22,23] Interestingly, the differences are similar to the situation on the adsorption of oxygen molecule on the Ge(001)[24] and Si(001) surfaces.[25]

TABLE 2: Calculated Adsorption Energies of the π-Complex Precursor (P), Transition (T), and Chemisorption (C) States for the Asymmetric Addition Pathways Displayed in Figure 2 and the Energy Barrier (E_b) from the P to the C States (All Data in electronvolts; for the Mixed Adsorption Cases, the Data Describe the Additional Adsorption so the Di-σ/End-Bridge Data Are for the Addition of End-Bridge Ethylene Next to Di-σ ethylene)

	calculated adsorption energies			
reaction path	P	T	C	E_b
di-σ	0.40	0.17	1.00	0.23
end-bridge	0.35	0.16	0.90	0.19
paired di-σ	0.23	0.06	0.97	0.17
paired-end-bridge	0.25	0.13	1.13	0.12
di-σ/end-bridge	0.22	0.08	0.81	0.14
end-bridge/di-σ	0.27	0.05	0.84	0.22

For the asymmetric addition route through the π-complex with a coverage up to 0.5 monolayer, the reaction barrier from the P_I state to the di-σ configuration is only 0.04 eV higher than the barrier from the P_{II} state to the end-bridge structure. If all the adsorption energy of the precursor states is retained, both formations of di-σ and end-bridge structure are actually barrierless. In other words, if the energy released by the formation of the precursor state is not dissipated away quickly, it is enough to drive the chemisorption through the first transition state. Hence, it is reasonable to expect both the di-σ and end-bridge configurations can be formed via this asymmetric route at most common experimental conditions. But at an extremely low temperature condition with rapid energy dissipation, the precursor state for the di-σ configuration formation may have a very long lifetime and the energy barrier of 0.23 eV is high enough to slow down the process of the di-σ configuration formation significantly relative to the rate of the end-bridge configuration formation. In comparison, if the surface temperature is high, since the adsorption energy of the P_I state is larger than that of the P_{II} state, the reaction rate to form the di-σ phase can be even higher than the reaction rate to form the end-bridge structure.

After studying the formation of the di-σ and end-bridge structure with the adsorption of one single molecule, we have also calculated the case of adding one more C_2H_4 molecule for the formation of the actual paired-di-σ and paired-end-bridge structure and found an adsorption energy of 0.23 and 0.25 eV for the precursor state and an energy barrier of 0.17 and 0.12 eV. Hence, both the addition of di-σ ethylene from 0.5 monolayer to the paired-di-σ adsorption at 1.0 monolayer and the homogeneous addition case for the formation of paired-end-bridge adsorption can proceed readily because of a small energy barrier.

As for the mixed adsorption cases, the respective energy barriers are 0.14 and 0.22 eV for the di-σ/end-bridge and end-bridge/di-σ adsorption. Hence, both cases can proceed easily too because the barriers are both small. At a low reaction temperature, obviously the addition of end-bridge adsorption is kinetically more favorable than the addition of di-σ adsorption. In fact, the energy barrier of the di-σ/end-bridge adsorption is also lower than both the di-σ/di-σ and end-bridge/di-σ adsorption; hence, at low temperature, the growth of di-σ adsorption is retarded and the end-bridge adsorption is dominating.

For the two mixed adsorption cases, the adsorption energies are 0.81 and 0.84 eV, which are ~0.2 eV less stable than the homogeneous adsorption. As such, unless the reaction temperature is low enough to preserve the random mixed adsorption as metastable configurations, phase separation to a mixture of di-σ domains and end-bridge domains is favorable.

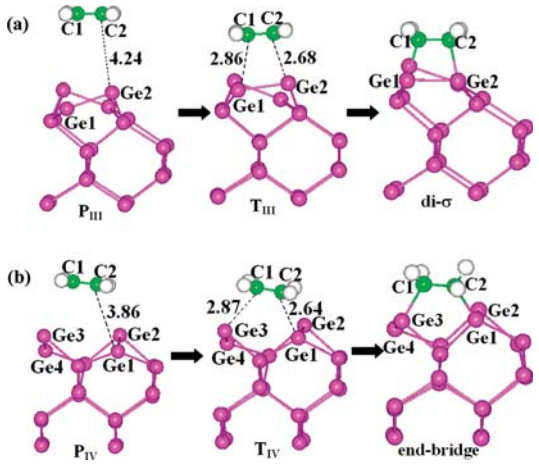

Figure 3. Atomic geometries of the physisorbed P, T, and C states for the adsorption of C_2H_4 on Ge(001) surface along (a) path III (concerted symmetric addition reactions leading to the di-σ structure) and (b) path IV (concerted symmetric addition reactions leading to the formation of the end-bridge structure).

TABLE 3: Calculated Adsorption Energies of the Physisorbed (P), Transition (T), and Chemisorption (C) states for the Symmetric Addition Pathways Displayed in Figure 3 and the Energy Barrier (E_b) from the P to the C States (All Data in electronvolts; for the Mixed Adsorption Cases, the Data Describe the Additional Adsorption so the Di-σ/End-Bridge Data Are for the Addition of End-Bridge Ethylene Next to Di-σ ethylene)

	calculated adsorption energy			
reaction path	P	T	C	E_b
di-σ	0.08	−0.09	1.00	0.17
end-bridge	0.11	0.06	0.90	0.05
paired-di-σ	0.08	−0.24	0.97	0.32
paired-end-bridge	0.10	0.0	1.13	0.1
di-σ/end-bridge	0.08	−0.01	0.81	0.09
end-bridge/di-σ	0.02	−0.24	0.84	0.26

3.2.3. Energetics of the Symmetric Reaction Pathways. Paths III and IV respectively describe the concerted symmetric addition pathways for the formation of the di-σ and end-bridge adsorption configurations. For the homogeneous adsorption to 0.5 monolayer, the physisorbed precursor states P_{III} and P_{IV} are displayed respectively in Figure 3a,b, with the respective adsorption energies of 0.08 and 0.11 eV. To form the di-σ (end-bridge) phase from the physisorbed precursor state P_{III} (P_{IV}), the C_2H_4 molecule should go over the transition state T_{III} (T_{IV}). The atomic geometries of the precursor, transition, and chemisorption states in paths III and IV are displayed in Figure 3a,b, and their adsorption energies are listed in Table 3. Along path III, transition state T_{III} has an adsorption energy of −0.09 eV and thus the energy barrier for the formation of the di-σ structure from physisorbed precursor state P_{III} is 0.17 eV. Along path IV, the adsorption energy of transition state T_{IV} is 0.06 eV and this gives an energy barrier of 0.05 eV for the formation of the end-bridge structure. Hence, for the symmetric addition to 0.5 monolayer, both di-σ and end-bridge adsorption can proceed easily because of their small energy barriers. At low temperature, the end-bridge adsorption is kinetically more favorable than the di-σ adsorption.

To study the formation of the actual paired-di-σ (paired-end-bridge) structure, we have also calculated the energy path of an additional C_2H_4 molecule on the di-σ (end-bridge) structure

via the concerted symmetric addition mechanism. In summary, the precursor states have respective adsorption energies of 0.08 and 0.1 eV, as displayed in Table 3. The data show that the energy barrier is 0.32 eV for the formation of paired-di-σ configuration that is much larger than the barrier of 0.17 eV for the formation of the di-σ configuration. Hence, once the di-σ adsorption reaches 0.5 monolayer, its growth to the paired-di-σ configuration will be retarded because of this higher energy barrier. In addition, this energy barrier is also significantly higher than the 0.1 eV barrier against the growth of the end-bridge adsorption to paired-end-bridge adsorption. Hence, in the context of concerted symmetric addition, di-σ and paired-end-bridge adsorption should also be the dominant surface phases.

For the mixed adsorption cases, the data in Table 3 also predict that the addition of end-bridge ethylene next to di-σ ethylene is more kinetically favorable that the addition of di-σ ethylene next to end-bridge ethylene. Once again, this condition will drive the paired-end-bridge adsorption to become the dominant surface phases.

3.2.4. Comparison of the Asymmetric and Symmetric Pathways. Among the asymmetric π-complex route and symmetric concerted [2 + 2] cyclo-addition route, although the concerted addition mechanism are not forbidden as we have discussed for the case on the Si(001) surface,[21] the asymmetric π-complex route is more accessible and more important since, unlike the concerted cyclo-addition route, the asymmetric π-complex route does not require the arrival of C_2H_4 with its molecular axis well-aligned with the Ge−Ge dimer and parallel to the surface. Thus, for most experimental conditions, the surface reactions are dominated by the formation of both the di-σ and end-bridge structures through the asymmetric π-complex route, enroute to the paired-di-σ and paired-end-bridge structures at 1.0 monolayer. On the whole, our calculation results explain the existence of the di-σ and paired-end-bridge structures which are the two adsorption geometries observed in the STM experiment and our reaction rate predictions are consistent with the population measurement of the two configurations.[8]

At an extremely low temperature, the precursor states of P_I and P_{II} via asymmetric addition will be the most probable surface adsorption structures due to their relatively deep potential wells (0.40 and 0.35 eV, respectively) and relatively high energy barriers to chemisorption (0.23 and 0.19 eV, respectively). Slowly the physisorption will proceed to chemisorption as the desorption energy is higher than the energy barrier to chemisorption. Since the end-bridge adsorption to 0.5 monolayer, the end-bridge/end-bridge adsorption, and the di-σ/end-bridge adsorption all have energy barriers lower than those for the di-σ adsorption to 0.5 monolayer, and end-bridge/di-σ adsorption, the end-bridge adsorption will be the dominant adsorption. By chance when the molecules arrive with the proper orientation for the concerted cyclo-addition route, the end-bridge formation channel is open with a barrier as little as 0.05 eV. As such, at an extremely low temperature, end-bridge adsorption via the concerted symmetric cyclo-addition can also proceed to chemisorption. But this route is still not the most probable one, in comparison to the end-bridge adsorption via asymmetric addition.

When the reaction temperature is raised, the di-σ adsorption channels become open for both asymmetric and symmetric additions. The probability of asymmetric addition remains much higher than symmetric addition due to the trajectory geometry consideration. Homogenous adsorption and mixed adsorption can both proceed, but the reaction rate to form the di-σ configuration can be even higher than the reaction rate to form the end-bridge configuration. When the temperature is relatively low, random mixed adsorption of di-σ and end-bridge can in principle generate a surface structure with virtually no ordering. The chemisorption states are metastable as the adsorption energy of all mixed adsorption cases are ~0.2 eV smaller than those of the homogeneous adsorption cases. Hence, when the temperature is further raised, phase separation leading to domain formation with some long-range ordering will occur.

3.3. Surface Band Structure. Parts b−e of Figure 4 show the surface band structure for the di-σ and end-bridge structure in the vicinity of E_F resulting from our calculation considering with 0.5 and 1.0 monolayer coverage. To track the surface states change induced by the adsorption of ethylene molecule, we also present the band structure of the bare Ge(001) $p(2 \times 2)$ surface. As shown in Figure 4a, the clean Ge(001) $p(2 \times 2)$ surface is observed to be semiconducting. The conduction band is 0.24 eV above the valence band, which is consistent with the previous angle-resolved photoemission spectroscopy and standing wave investigations[26] where the surface conduction band is 0.3 eV above the valence band.

At 0.5 monolayer coverage of ethylene on Ge(001), the band gap of both the di-σ and end-bridge structures widen to 0.36 eV as indicated in Figure 4b,c, and there are still two surface states in the band gap region. Most importantly, both the two band structures have the semiconducting character. Hence, our band structure calculations disagree with the previously reported calculation results that indicate the band structure of the end-bridge configuration for both C_2H_4/Ge(001) and C_2H_4/Si(001) is metallic.[9]

When the coverage increases to 1.0 monolayer, the energy gaps of the two adsorption models increase further, as shown in Figure 4d,e, which are 0.81 and 0.46 eV for the paired-di-σ structure and paired-end-bridge structure, respectively. There is no surface state in the gap region anymore. In other words, the detrimental issue of Fermi level pinning is clear by increasing the ethylene dosage to the full coverage condition. Obviously this clearance of surface states in the band gap means that adsorption of ethylene to the full-coverage condition can be exploited as a means of surface passivation of Ge(001) in device fabrication.

The electronic band structures of the mixed adsorption products of Figure 1e,f are shown in Figure 4f; the surface states in the gap region are more than the surface states in Figure 4b,c. The band gaps of the two mixed configurations are slightly widened to ~0.30 eV, which are smaller than those of the di-σ and end-bridge configurations at 0.5 monolayer.

3.4. Surface States in the Vicinity of Fermi Energy. To investigate the origin of the surface states, we decompose the Ge 4p and C 2p density of states (DOS) into its p_x, p_y, and p_z symmetry components in Figure 5a−e. The local DOS of the bare Ge(001)$p(2 \times 2)$ surface is displayed in Figure 5a, with the upper and lower panels of Figure 5a referring to the upper and lower Ge atom of the tilted dimer, respectively. Considering the fact that the Ge(001) surface is on the xy plane with the surface dimer axis along the x direction in our calculations, one can easily see that the p_z orbital is perpendicular to the surface. Comparing the decomposed DOS of the upper and lower Ge atoms, we find that the unoccupied dangling bond state is mainly from the lower atom, while the occupied dangling bond state is dominated by the upper atom. This is supported by the fact that there is a net electron transfer from the low atom to the up atom due to the buckling of the dimer. It is worthy noting that there is a small contribution of the p_y atomic orbital mainly from the lower atom which is much closer to E_F than the occupied dangling bond states. These p_y atomic orbitals should contribute

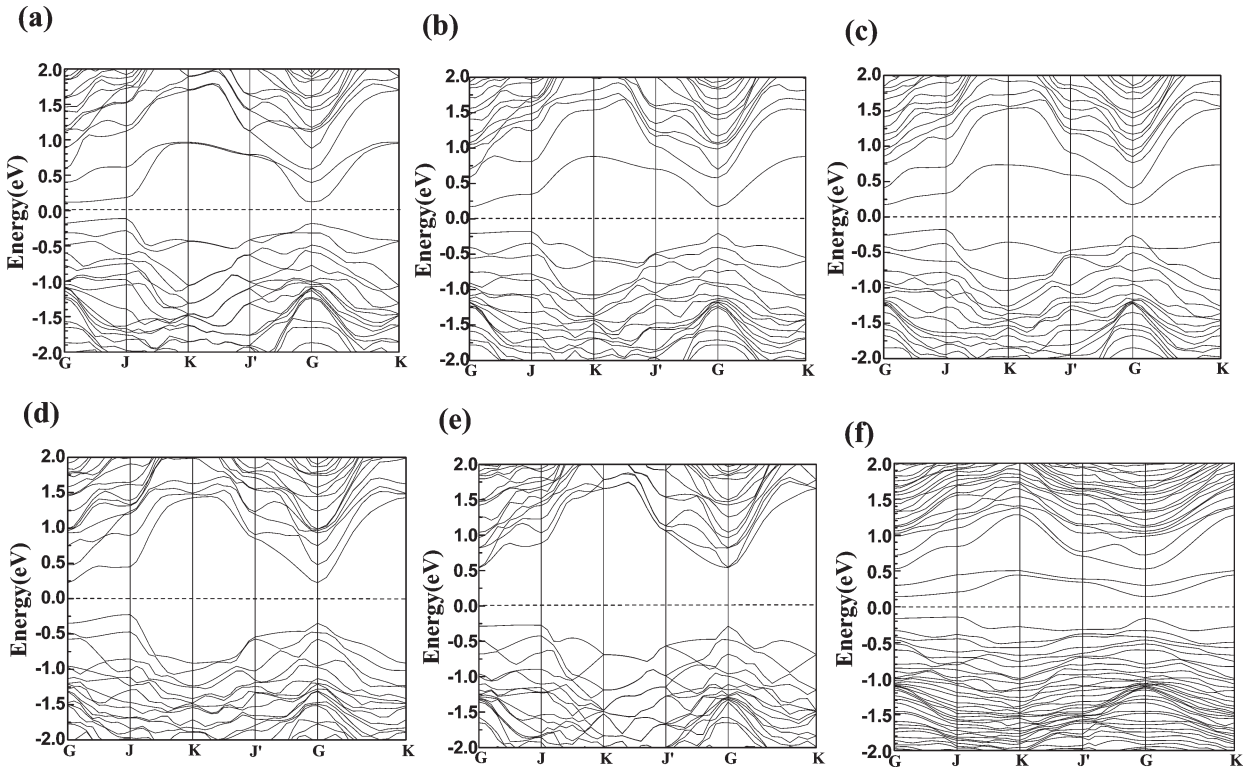

Figure 4. Electronic band structures of the (a) clean Ge(001) $p(2 \times 2)$ surface, (b) di-σ C_2H_4/Ge(001) at 0.5 monolayer, (c) end-bridge C_2H_4/Ge(001) at 0.5 monolayer, (d) paired-di-σ C_2H_4/Ge(001) at 1.0 monolayer, (e) paired-end-bridge C_2H_4/Ge(001) at 1.0 monolayer, and (f) mixed di-σ and end-bridge C_2H_4/Ge(001) at 0.5 monolayer.

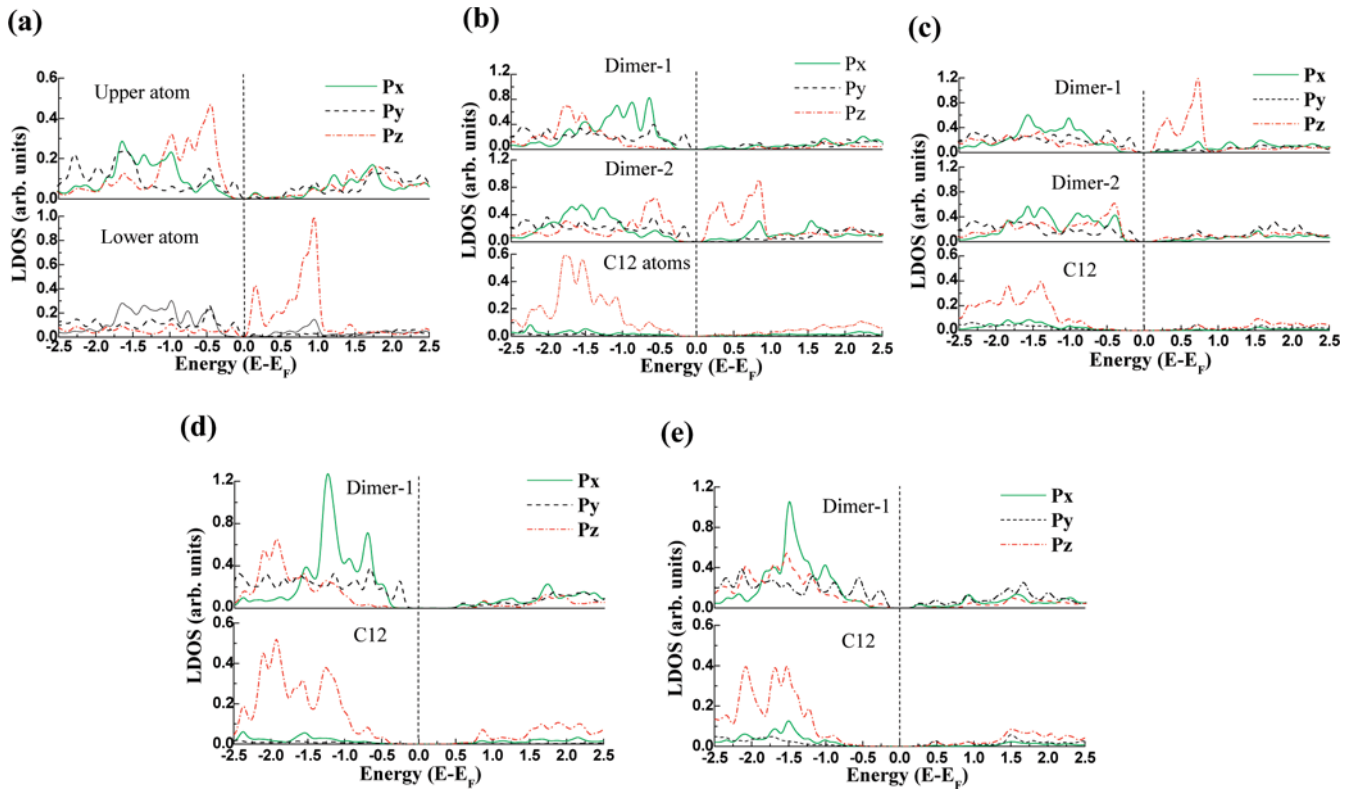

Figure 5. Decomposed local density states of the (a) clean Ge(001) $p(2 \times 2)$ surface, (b) di-σ C_2H_4/Ge(001) at 0.5 monolayer, (c) end-bridge C_2H_4/Ge(001) at 0.5 monolayer, (d) paired-di-σ C_2H_4/Ge(001) at 1.0 monolayer, and (e) paired-end-bridge C_2H_4/Ge(001) at 1.0 monolayer.

to the back-bond surface state. In this context, the previous experimental studies[26] found that the top valence band of the Ge(001) surface at Γ point is mainly derived from a bulk state, but one recent STM experiment[27] confirmed that the top of the valence band on Ge(001) is the back-bond state, while in the previous LDOS calculation for the Ge(001) surface by Schwingerschlogl and Schuster[28] the Ge 4P DOS was also decomposed into three symmetry components. In the vicinity of Fermi energy, almost all of the states have symmetry perpendicular to the surface, which will contribute to dangling bond states.

Another symmetry component along the dimer axis which will contribute to the back-bond states is found to be negligible. Thus, they drew the conclusion that the highest occupied surface states are the dangling bond states not the back-bond states. Our LDOS calculation results reveal the origin of highest occupied states reported in the photoemission[26] and STM studies.[27]

The decomposed Ge 4p and C 2p DOS for the di-σ structure are shown in Figure 5b, where dimer-1 in the upper panel and dimer-2 in the lower panel refer to the dimer with and without ethylene adsorption, respectively. The LDOS of dimer-1 indicates that the occupied and unoccupied dangling bond states disappear due to the saturation of the Ge atoms, while, for the LDOS of dimer-2, the surface states are almost the same as those on the bare surface. For the end-bridge structure in Figure 5c, because the ethylene molecule is only bonded to one Ge atom of each dimer, the unoccupied dangling bond state on dimer-1 still exists while the occupied dangling bond state disappears. In comparison, the unoccupied dangling bond state of dimer-2 disappears while the occupied dangling bond state still exists. Especially, for both the di-σ and end-bridge structures, the small contribution of the p_y component changes little from the original bare surface. Our partial change density calculations confirm that the surface states of the top valence band within -0.2 eV below the E_F is the back-bond states. Furthermore, for both the band structures of the di-σ and end-bridge configuration as displayed in Figure 4b,c, there are two states just below and above the E_F. Obviously the origin of these two states can be investigated from the decomposed LDOS in Figure 5b,c, which indicates the two states are mainly from the occupied and unoccupied dangling bond states localized on the Ge atom without adsorption. Once again, our result does not support the conclusion drawn by Miotto et al.[9] where they assigned the highest occupied state of di-σ configuration to the adsorbed ethylene molecule. Actually, when an ethylene molecule adsorbs on a Ge−Ge dimer, the binding interaction is between the frontier orbital of both. It is well-known that the occupied binding orbital will decrease in energy, which is clear in the LDOS for all four adsorption configurations. As shown in Figure 5b−e, the obvious LDOS of the ethylene molecule appears at 1.0 eV below the Fermi level. Thus, the major contribution of the highest occupied states cannot be the ethylene molecule.

At the coverage of 1.0 monolayer, the LDOS of paired-di-σ and paired-end-bridge configurations are similar to each other, and all of the unoccupied and occupied dangling bond states disappear due to the saturation of Ge atoms by ethylene adsorption. Once again, the LDOS calculations show the small contribution of the p_y component within -0.3 eV below E_F, which indicates that the highest occupied states are still the back-bond states. In our previous study for the adsorption of oxygen molecule on Ge(001) surface,[24] the back-bond surface state changes little during the nondissociative adsorption of the oxygen molecule, which is similar to the present situation of ethylene adsorption.

We have also calculated the LDOS for the two mixed adsorption configurations, the decomposed Ge 4p and C 2p DOS of the unreacted dimer; the di-σ ethylene and the dimer under it are similar to those in Figure 5b, while the decomposed Ge 4p and C 2p DOS of the end-bridge ethylene and the two dimers under it are similar to those in Figure 5c.

4. Conclusions

Six possible adsorption configurations for C_2H_4/Ge(001) have been investigated. At 0.5 monolayer, the di-σ configuration is more stable than the end-bridge configuration, and the two mixed adsorption configurations of adding di-σ ethylene next to end-bridge ethylene and adding end-bridge ethylene next to di-σ ethylene near each other are both $\sim$0.2 eV less stable than the homogeneous di-σ adsorption. However, the end-bridge adsorption is kinetically more favorable than the di-σ adsorption. For the adsorption to 1.0 monolayer, the paired-end-bridge configuration is both thermodynamically more stable and kinetically more favorable than the paired-di-σ configuration. Mixed adsorption leading to the domains of the paired-end-bridge configuration is also expected. Most adsorption products are formed by asymmetric addition, but the symmetric addition can also proceed as it is limited only by the special trajectory geometry requirement rather than by the presence of any high energy barrier. At extremely low temperature, the end-bridge adsorption will be the dominant adsorption process, while, at high temperature, the formation rate of the di-σ structure is larger than that of the end-bridge structure which will be easily proceeded to form the paired-end-bridge structure.

Our band structure calculation results show that the di-σ and end-bridge configuration at 0.5 monolayer have the semiconducting character with a slightly increased energy gap. The band gap further increases when the coverage reaches 1.0 monolayer. These results thus rule out the past postulation that ethylene adsorption may turn Ge(001) to metallic. On the basis of the analysis of the decomposed LDOS in the di-σ and end-bridge configuration, we attribute the surface states in the band gap region to the Ge atom, which denies the previous claim that the highest occupied state on the band structure of the di-σ configuration comes from the absorbed molecule.

Acknowledgment. We thank Professor Zhifeng Liu and Doctor Keisuke Sagisaka for valuable discussion. This work was funded by the Discovery Grant program of the Natural Science and Engineering Research Council of Canada (NSERC) for W.M.L., the National Natural Science Foundation of China (NSFC; Grant 20773024) for Y.F.Z., and funds from Shannxi Province (Grant SJ08B14) and NSFC (Grant 20903075) for X.L.F. This work was also supported by the 111 Project in China. We also acknowledge the support from the Surface Science Western and the Faculty of Science at the University of Western Ontario.

References and Notes

(1) Wolkow, R. A. *Annu. Rev. Phys. Chem.* **1999**, *50*, 413.
(2) Mayne, A. J.; Avery, A. R.; Knall, J.; Jones, T. S.; Briggs, G. A. D.; Weinberg, W. H. *Surf. Sci.* **1993**, *284*, 247.
(3) Matsui, F.; Yeom, H. W.; Matsuda, I.; Ohta, T. *Phys. Rev. B* **2000**, *62*, 5036.
(4) Hennies, F.; Fohlisch, A.; Wurth, W.; Witkowski, N.; Nagasono, M.; Piancastelli, M. N. *Surf. Sci.* **2003**, *529*, 144.
(5) Widdra, W.; Fink, A.; Gokhale, S.; Trischberger, P.; Menzel, D.; Birkenheuer, U.; Gutdeutsch, U.; Rösch, N. *Phys. Rev. Lett.* **1998**, *80*, 4269.
(6) Xu, S. H.; Keeffe, M.; Yang, Y.; Chen, C.; Yu, M.; Lapeyre, G. J.; Rotenberg, E.; Denlinger, J.; Yates, J. T. *Phys. Rev. Lett.* **2000**, *84*, 939.
(7) Marsili, M.; Witkowski, N.; Pulci, O.; Pluchery, O.; Silverstreli, P. L.; Sole, R. D.; Borensztein, Y. *Phys. Rev. B* **2008**, *77*, 125337.
(8) Kim, A.; Choi, D. S.; Lee, J. Y.; Kim, S. *J. Phys. Chem. B* **2004**, *108*, 3256.
(9) Miotto, R.; Ferraz, A. C.; Srivastava, G. P. *Surf. Sci.* **2002**, *507*, 12.
(10) Cho, J. H.; Morikawa, Y. *J. Chem. Phys.* **2006**, *124*, 024716.
(11) Kresse, G.; Hafner, J. *Phys. Rev. B* **1993**, *47*, R558.
(12) Kresse, G. Hafner. *J. Phys. Rev. B* **1994**, *49*, 14251.
(13) Kresse, G.; Furthmüller, J. *Phys. Rev. B* **1996**, *54*, 11169.
(14) Kresse, G.; Furthmüller, J. *Comput. Mater. Sci.* **1996**, *6*, 15.
(15) Vanderbilt, D. *Phys. Rev. B* **1990**, *41*, 7892.
(16) Cohen, M. L. *Phys. Rep.* **1984**, *110*, 293.
(17) Payne, M. C.; Teter, M. P.; Allan, D. C.; Arias, T. A.; Joannopoulos, J. D. *Rev. Mod. Phys.* **1992**, *64*, 1045.

(18) Perdew, J. P. In *Electronic Structure of Solids '91*; Ziesche, P., Eschrig, H., Eds.; Academie-Verlag: Berlin, 1991; p 11.

(19) Jónsson, H. *Annu. Rev. Phys. Chem.* **2000**, *51*, 623.

(20) Henkelman, G.; Uberuaga, B. P.; Jónsson, H. *J. Chem. Phys.* **2000**, *113*, 9901.

(21) Fan, X. L.; Zhang, Y. F.; Lau, W. M.; Liu, Z. F. *Phys. Rev. B* **2005**, *72*, 165305.

(22) Zhang, Q. J.; Fan, X. L.; Lau, W. M.; Liu, Z. F. *Phys. Rev B* **2009**, *79*, 195303.

(23) Cho, J. H.; Kleinman, L.; Chan, C. T.; Kim, K. S. *Phys. Rev. B* **2001**, *63*, 073306.

(24) Fan, X. L.; Lau, W. M.; Liu, Z. F. *J. Phys. Chem. C* **2009**, *113*, 8786.

(25) Fan, X. L.; Lau, Zhang, Y. F.; W, M.; Liu, Z. F. *Phys. Rev. Lett.* **2005**, *94*, 016101.

(26) Nakatsuji, K.; Takagi, Y.; Komori, F.; Kusuhara, H.; Ishii, A. *Phys. Rev. B* **2005**, *72*, 241308.

(27) Radny, M. W.; Schofiled, G. A.; Smith, P. V.; Curson, N. J. *Phys. Rev. Lett.* **2008**, *100*, 246807.

(28) Schwingerschlogl, U.; Schuster, C. *Chem. Phys. Lett.* **2007**, *449*, 126.

JP9086464